ChemComm

Accepted Manuscript

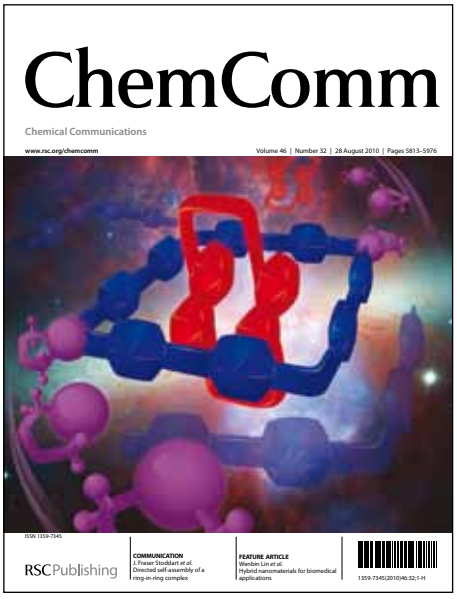

This is an *Accepted Manuscript*, which has been through the RSC Publishing peer review process and has been accepted for publication.

Accepted Manuscripts are published online shortly after acceptance, which is prior to technical editing, formatting and proof reading. This free service from RSC Publishing allows authors to make their results available to the community, in citable form, before publication of the edited article. This *Accepted Manuscript* will be replaced by the edited and formatted *Advance Article* as soon as this is available.

To cite this manuscript please use its permanent Digital Object Identifier (DOI®), which is identical for all formats of publication.

More information about *Accepted Manuscripts* can be found in the **Information for Authors**.

Please note that technical editing may introduce minor changes to the text and/or graphics contained in the manuscript submitted by the author(s) which may alter content, and that the standard **Terms & Conditions** and the **ethical guidelines** that apply to the journal are still applicable. In no event shall the RSC be held responsible for any errors or omissions in these *Accepted Manuscript* manuscripts or any consequences arising from the use of any information contained in them.

Journal Name

RSCPublishing

COMMUNICATION

A molecular rotor for measuring viscosity in plasma membranes of live cells

Cite this: DOI: 10.1039/xoxxoooooox

Ismael López-Duarte,[a#] Thanh Truc Vu,[a#] M. Angeles Izquierdo,[a] James A. Bull [a] and Marina K. Kuimova [a*]

Received ooth January 2012,
Accepted ooth January 2012

DOI: 10.1039/xoxxoooooox

www.rsc.org/

Molecular rotors have emerged as versatile probes for microscopic viscosity in live cells, however, the exclusive localisation of rotors in the plasma membrane has remained elusive. We report the synthesis, spectroscopic characterisation and live cell imaging of a new BODIPY-based molecular rotor suitable for mapping viscosity in the cell plasma membrane.

Measuring viscosity in biological systems is of paramount importance for the understanding of biophysical processes governing both the normal cell function and the cell demise. This important challenge has been successfully addressed by the application of spectroscopic techniques, which are alone capable of probing the viscosity and diffusion on the length scales of single biological cells and organelles, down to the level of individual membrane domains. Molecular rotors, which report on variations in viscosity by changes in their fluorescence intensity or lifetime have been at the forefront of recent developments in measuring intracellular viscosity.[1, 2] In this class of fluorophores the non radiative decay of the excited state displays an extremely strong dependence on the viscosity of their immediate micro-environment, which allows precise calibration of fluorescence parameters with viscosity. This in turn allows spatially resolved imaging of viscosity in live cells, using the lifetime-based or ratiometric approach to counteract the uncertainties in the fluorophore's concentration. Several such molecular rotors suitable for imaging of viscosity of internal cellular organelles have been reported,[3-9] including specific probes for lysosomes[10] and mitochondria[11] as well as genetically targeted probes.[12] On the other hand, a probe to exclusively target the cellular plasma membrane has not been available, in spite of the paramount importance of membrane viscosity in cellular processes. Such a probe is highly desirable due to the key role that membrane fluidity is thought to play in protein-protein interactions (*e.g. via* the formation of lipid rafts), in the action of anaesthetics and other drugs, in disease development (*e.g. via* the formation of insoluble plaques), in resistance to shear stress, and more generally in any processes that require diffusion of reagents within and across the membrane bilayer.[1, 2, 13]

While specially designed membrane-soluble molecular rotors have been successfully used for viscosity probing in model lipid bilayers[14, 15] and monolayers,[16] the imaging of the plasma membrane in live cells was not possible due to the effective endocytosis of the dyes inside live cells.[3, 4, 8] As a consequence, probes such as BODIPY-C_{12} (**1**, Fig. 1) were only able to report on the viscosity of the lipid membranes of internal cellular organelles.[3, 4] Here we report the design and detailed characterisation of the molecular rotor **2**, which is effectively prevented from endocytosis by the double positive charge located on its hydrocarbon tail.

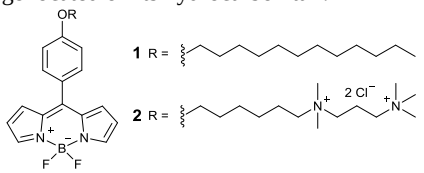

Fig. 1 Molecular structures of BODIPY **1** and **2**.

The model molecular rotor **1,** based on the BODIPY structure, is sensitive to viscosity, as determined by the ease of the rotation of the *meso*-phenyl group in different environments. Efficient rotation opens access to a dark non-emissive state in which the emission is quenched. We have previously demonstrated that both the fluorescence quantum yield, Φ_f, and lifetime, τ_f, of **1** increases dramatically with increasing viscosity, in a large viscosity range 10-5000 cP,[15] consistent with the Förster-Hoffmann equation[17] (1)

$$\Phi_f = z\eta^{\alpha} \quad (1)$$

where z and α are constants, η is viscosity.

For measurements that are free from the bias of variable concentration of the dye in a heterogeneous sample, it is more convenient to use τ_f instead of the fluorescence intensity. Fluorescence decay in a heterogeneous sample can be measured in a spatially resolved manner using a Fluorescence Lifetime Imaging (FLIM) approach. We can rewrite the Förster-Hoffmann equation for τ_f, Equation (2).[1, 3]

$$\tau_f = \frac{z\eta^{\alpha}}{k_r} \quad (2)$$

where k_r is the radiative decay rate constant.

The rotor **1** was initially designed as a FLIM viscosity probe for lipid bilayers. However, we did not succeed in staining the plasma membrane of the cell with **1** due to its internalisation, even at a low incubation temperature and with short incubation times. No membrane staining was recorded even by incubating live cells with **1**

Chemical Communications Accepted Manuscript

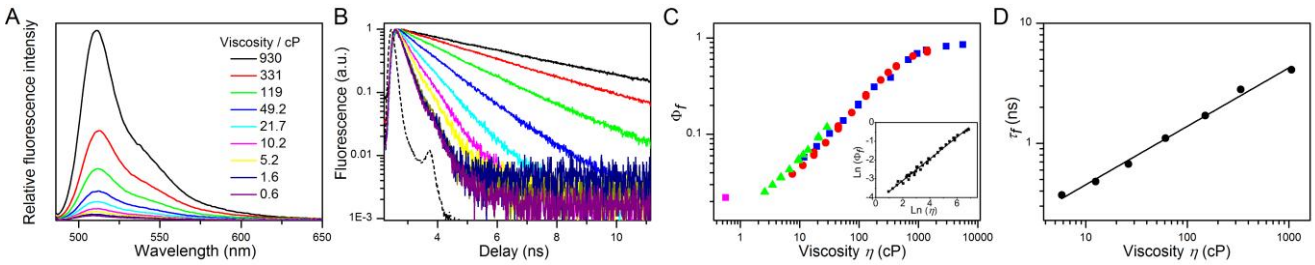

Fig. 2 Fluorescence characterisation of **2** in methanol/glycerol mixtures of varied viscosity. (A) Fluorescence spectra; (B) Time resolved fluorescence decays, the viscosity values are colour coded as in (A), the dotted line corresponds to the IRF; (C) Fluorescence quantum yield recorded at varied temperatures 5-100 °C; % glycerol: ■ 100; • 90; ▲ 50; ■ 0. Inset: the calibration graph according to Equation (1); (D) The calibration graph of τ_f *vs* η according to Equation (2).

at the microscope stage and continuously monitoring cell uptake from time zero.[4] Here we hypothesised that adding a double positive charge on the hydrocarbon tail of **1** would prevent efficient endocytosis, while retaining the rotor function, to produce the derivative **2**, Fig. 1. This strategy was previously used to achieve the plasma membrane staining of dyes useful for second harmonic generation (SHG) imaging.[18, 19]

Preparation of BODIPY **2** can be achieved as shown in Scheme 1 (see ESI for full synthetic and characterisation details of compounds **2**, **3** and **4**). Firstly, BODIPY **3** was synthesised by modification of established literature procedures.[20] Following characterization, **3** was reacted with an excess of *N,N,N′,N′*-tetramethyl-1,3-propanediamine in THF to afford the corresponding mono charged derivative which precipitated out of the reaction medium. This intermediate, which was not isolated, was further reacted with iodomethane in DMF. Chromatographic purification and anion exchange, afforded BODIPY **2** and the structure was confirmed by NMR spectroscopy and mass spectrometry. The resulting BODIPY **2** is well soluble in water as well as in a range of organic solvents.

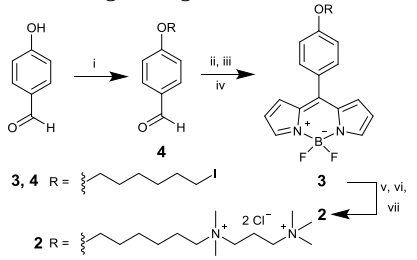

Scheme 1 Synthesis of BODIPY **2**: (i) 1,6-diiodohexane, K_2CO_3, DMF; (ii) neat pyrrole, TFA; (iii) DDQ, CH_2Cl_2; (iv) $BF_3(OEt_2)_2$, Et_3N, CH_2Cl_2; (v) *N,N,N′,N′*-Tetramethyl-1,3-propanediamine, THF, RT; (vi) CH_3I, DMF, RT; (vii) Dowex® 1×8 200 mesh ion-exchange column, H_2O.

BODIPY **2** displays absorption and emission spectra similar to **1** (Fig. S6, ESI). We confirmed that **2** acts as a molecular rotor by measuring fluorescence emission spectra in methanol-glycerol mixtures of varied viscosity, Fig. 2A. As expected for a molecular rotor, emission quantum yield of **2** increases strongly (*ca* 39 fold) upon viscosity increase from 0.5 to 5600 cP, Fig. 2C. We repeated the measurements in several mixtures (50, 90 and 100% glycerol) at a range of temperatures between 5-100 °C to *(i)* extend the viscosity range available to us and *(ii)* verify that the data recorded for samples at different temperatures and compositions but equal viscosity display identical quantum yields.

We observed a good overlap between different temperature and composition data, Fig. 2C. Based on this data we concluded that the main determinant of the photophysical properties of **2** is, indeed, viscosity and thus this viscosity probe retains its calibration at different temperatures (Fig. S7 gives a calibration plot where the temperature was taken into account). The viscosity range where the quantum yield of the probe increases according to the Förster-Hoffmann equation (1) is *ca* 3-1000 cP, and the linearity (and the sensitivity to viscosity) is lost below and above this range**,** reflecting the range of sensitivity of k_{nr} of **2** to viscosity. We note that the polarity effect on the photophysics of **2** is minimal, Fig. S8. These observations are similar to those previously reported for **1**.[15] Likewise, as expected from Equation (2), the fluorescence decays of **2** show strong dependence on viscosity, Fig. 2B. The decays are single exponential and conform to Equation (2) to create the calibration graph of fluorescence lifetime *vs* viscosity (Fig. 2D).

Next, we have tested the uptake of **2** in live cells (see ESI for detailed protocols). Best results in the plasma membrane staining were obtained when, prior to imaging, SK-OV-3 cells were incubated in a 8.9 μM dye solution at 4 °C with Mg^{2+} and Ca^{2+} free medium, in order to slow down endocytosis. Under these conditions, the dye membrane uptake is fast, and the dye exclusively stains the plasma membranes of SK-OV-3 cells, at least at incubation times <30 min (Fig. 3), which are sufficient for FLIM image acquisition. At longer times (*e.g.* 55 min, Fig. 3C, D, Fig. S11) or upon incubation at room temperature in standard media (Fig. S12), internal staining of cells becomes evident, along with persistent and clear plasma membrane staining. To the best of our knowledge, this is the first example of a molecular rotor which selectively internalises into plasma membranes.

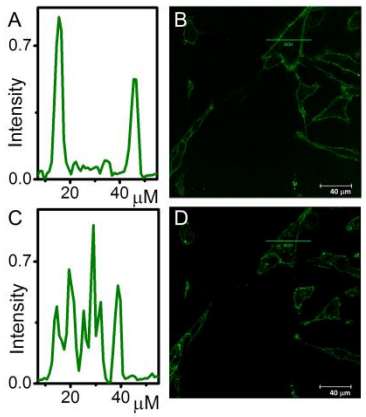

Fig. 3 Confocal images of SK-OV-3 cells recorded 9 min (A, B) and 55 min (C, D) following the incubation of a fresh layer of cells with 8.9 μM solution of **2**. Panels A and C show the fluorescence intensity profiles across a single cell indicated by a bar in the image.

We have recorded FLIM of SK-OV-3 cells stained with **2**, Fig. 4. All the decays in the image could be fitted using a single exponential algorithm, with a good χ^2. The lifetime histogram is of a nearly Gaussian shape, with the maximum at 2.2 ns (Fig. S9, ESI). We note that the large full width half maximum (FWHM) of this histogram truly reflects the heterogeneity of the cellular membrane rather than

Chemical Communications Accepted Manuscript

 This journal is © The Royal Society of Chemistry 2012

a low measurement accuracy, as demonstrated by the very low FWHM, recorded from homogeneous solutions (Fig. S10, Table S1).

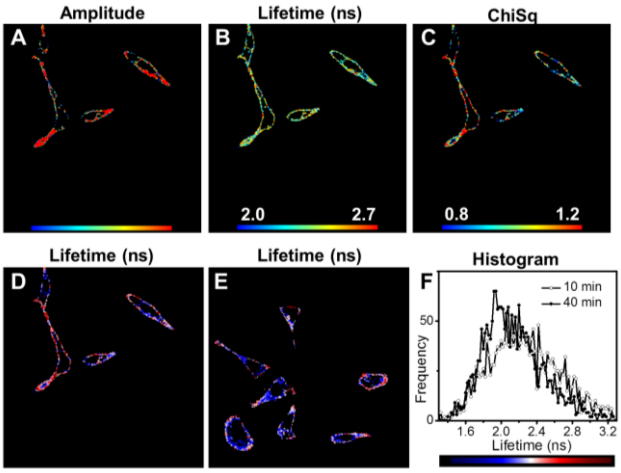

Fig. 4 Fluorescence imaging of SK-OV-3 cells incubated with 8.9 μM solution of BODIPY **2** obtained following 990 nm pulsed excitation and [510-700] nm fluorescence detection. A: Two-photon fluorescence image, 228 × 228 μm; B, D, E: FLIM images, B: lifetime range from 2.0 to 2.7 ns; D and E: lifetime range from 1.3 to 3.3 ns; C: ChiSq (goodness of fit) image, $0.8< \chi^2 <1.2$; F: Lifetime histograms obtained from D and E and a seismic colour scale used to assign the lifetimes in the images D and E.

According to our lifetime calibration graph (Fig. 2D), this value corresponds to a viscosity of *ca* 270 cP.

We have also recorded FLIM images of cells incubated with **2** for 40 minutes that show some staining of internal organelles, Fig. 4E. The histogram recorded from this image is shifted to lower lifetimes compared to that of the 10 min incubation sample, Fig. 4F. Moreover, this histogram is better described by a bimodal Gaussian fit (Fig. S7, ESI). We have assigned a seismic colour scale to these histograms, such that all pixels with lifetimes below 2.3 ns are coloured blue, while those with lifetimes above 2.3 ns are red. It is clear to see that the plasma membrane in both images (10 and 40 min incubation) is characterised by a red colour (longer lifetime) while the internal stained organelles are coloured blue (Fig. 4 D-F).

Based on a bimodal fitting of the histogram for the 40 min image, we can assign average viscosities to both cellular domains probed by the rotor: *ca* 200 cP (1.9 ns) for internal organelles and *ca* 270 cP (2.2 ns) for the plasma membrane. Thus the plasma membrane viscosity measured here exceeds the viscosity of the lipid-rich environment of the internal cellular organelles. The viscosity of internal SK-OV-03 organelles measured previously with rotor **1** was *ca* 160 and 200 cP (two domains detected). These values are consistent with those detected in the current study.

The values recorded for the plasma membrane by **2** are higher than those for the internal staining, and this trend is consistent with the results of a recent molecular rotor study.[9] At the same time they are considerably lower than those recorded by us with **1** for the L_o phase in model membranes (600-800 cP)[15] and also lower than 600 cP reported for the plasma membrane in the recent study.[9] The difference in these values can be due to *(i)* the variations in rotor localisation through the thickness of the bilayer or *(ii)* the less efficient staining of L_o phase in the plasma membrane by our rotor **2**.

In conclusion, we have reported the first viscosity sensitive molecular rotor which selectively stains the plasma membranes of live cells. Further developments in rotor design might allow for the distinguishing of plasma membrane domains and detecting variations in membrane fluidity upon application of external stimuli.

MKK and JAB are thankful to the EPSRC for Career Acceleration Fellowships. This work was partially supported by the European Commission in the form of Marie Curie individual Fellowships to TTV and MAI.

Notes and references

[a] *Chemistry Department, Imperial College London, Exhibition Road, South Kensington, SW7 2AZ, United Kingdom; m.kuimova@imperial.ac.uk*

[#] These authors contributed equally.

† Electronic Supplementary Information (ESI) available: detailed synthetic procedures and compound characterisation, experimental details and additional spectroscopic/imaging data. See DOI: 10.1039/c000000x/

1. M. K. Kuimova, *Phys. Chem. Chem. Phys.*, 2012, **14**, 12671-12686.
2. M. A. Haidekker and E. A. Theodorakis, *Org. Biomol. Chem.*, 2007, **5**, 1669-1678.
3. M. K. Kuimova, G. Yahioglu, J. A. Levitt and K. Suhling, *J. Am. Chem. Soc.*, 2008, **130**, 6672-6673.
4. J. A. Levitt, M. K. Kuimova, G. Yahioglu, P.-H. Chung, K. Suhling and D. Phillips, *J. Phys. Chem. C*, 2009, **113**, 11634-11642.
5. K. Luby-Phelps, S. Mujumdar, R. B. Mujumdar, L. A. Ernst, W. Galbraith and A. S. Waggoner, *Biophys. J.*, 1993, **65**, 236-242.
6. X. Peng, Z. Yang, J. Wang, J. Fan, Y. He, F. Song, B. Wang, S. Sun, J. Qu, J. Qi and M. Yang, *J. Am. Chem. Soc.*, 2011, **133**, 6626-6635.
7. M. K. Kuimova, S. W. Botchway, A. W. Parker, M. Balaz, H. A. Collins, H. L. Anderson, K. Suhling and P. R. Ogilby, *Nat. Chem.*, 2009, **1**, 69-73.
8. M. A. Haidekker, T. T. Ling, M. Anglo, H. Y. Stevens, J. A. Frangos and E. A. Theodorakis, *Chem. Biol.*, 2001, **8**, 123-131.
9. A. Battisti, S. Panettieri, G. Abbandonato, E. Jacchetti, F. Cardarelli, G. Signore, F. Beltram and R. Bizzarri, *Anal. Bioanal. Chem.*, 2013, **405**, 6223-6233.
10. L. Wang, Y. Xiao, W. Tian and L. Deng, *J. Am. Chem. Soc.*, 2013, **135**, 2903-2906.
11. Z. Yang, Y. He, J.-H. Lee, N. Park, M. Suh, W.-S. Chae, J. Cao, X. Peng, H. Jung, C. Kang and J. S. Kim, *J. Am. Chem. Soc.*, 2013, **135**, 9181-9185.
12. E. Gatzogiannis, Z. Chen, L. Wei, R. Wombacher, Y.-T. Kao, G. Yefremov, V. W. Cornish and W. Min, *Chem. Commun.*, 2012, **48**, 8694-8696.
13. M. A. Haidekker, N. L'Heureux and J. A. Frangos, *Am. J. Physiol.-Heart C.*, 2000, **278**, H1401-H1406.
14. M. E. Nipper, M. Dakanali, E. Theodorakis and M. A. Haidekker, *Biochimie*, 2011, **93**, 988-994.
15. Y. Wu, M. Stefl, A. Olzynska, M. Hof, G. Yahioglu, P. Yip, D. R. Casey, O. Ces, J. Humpolickova and M. K. Kuimova, *Phys. Chem. Chem. Phys.*, 2013, **15**, 14986-14993.
16. N. A. Hosny, G. Mohamedi, P. Rademeyer, J. Owen, Y. Wu, M.-X. Tang, R. J. Eckersley, E. Stride and M. K. Kuimova, *Proc. Natl. Acad. Sci. U. S. A.*, 2013, **110**, 9225-9230.
17. T. Förster and G. Hoffmann, *Z. Phys. Chem. (N. F.)*, 1971, **75**, 63-69
18. L. Jin, A. C. Millard, J. P. Wuskell, X. M. Dong, D. Q. Wu, H. A. Clark and L. M. Loew, *Biophys. J.*, 2006, **90**, 2563-2575.
19. J. E. Reeve, H. L. Anderson and K. Clays, *Phys. Chem. Chem. Phys.*, 2010, **12**, 13484-13498.
20. A. Loudet and K. Burgess, *Chem. Rev.*, 2007, **107**, 4891-4932.

Chemical Communications Accepted Manuscript